OPEN EUROPEAN JOURNAL ON VARIABLE STARS
July 2023 http://oejv.physics.muni.cz ISSN 1801-5964
DOI: 10.5817/OEJV2023-0239

Time-series Photometry and Analysis of the BY Draconis Class Star: GSC 05586-00270

BRINCAT M STEPHEN [1,6], GALDIES, CHARLES [2,6]; GRECH WINSTON [3]; HILLS KEVIN [4,6]; MIFSUD MARTIN [5,6]

1) Flarestar Observatory (MPC 171), Fl. 5/B, George Tayar Street, San Gwann, SGN 3160, Malta, stephenbrincat@gmail.com
2) Institute of Earth Systems, University of Malta, MSD2080, Malta, charles.galdies@um.edu.mt
3) Antares Observatory, 76/3, Kent Street, Fgura FGR 1555, Malta, win.grech@gmail.com
4) Tacande Observatory, El Paso, La Palma, Spain, kevinhills@me.com
5) Manikata Observatory, Manikata, Malta, mifsudm0@gmail.com
6) American Association of Variable Star Observers

Abstract: This study investigates GSC 05586-00270 (a BY Draconis star) through data obtained from the ASAS-SN survey and additional observations from several observatories in Malta and another at La Palma (Spain). The study reveals the star's multi-period variability, with a primary period of 9.098805 ± 0.001507 days. Our analysis demonstrates that the primary period is relatively stable. Data analysis also divulged occasional fading and systematic variations in brightness and colour as the star undergoes rotation coupled with phenomena emanating from magnetic activity. A long-term period of approximately 4442 days was also identified, suggesting potential star spot migration influenced by other external factors. As opposed to some BY Draconis stars that are single, our analysis indicates that GSC 05586-00270 is likely to be a binary star system, influencing further the star's brightness variations. These findings shed light on the dynamic nature of this star and highlight the need for more comprehensive research to understand its behaviour further.

1 Introduction

BY Draconis stars, also known as BY Draconis variables or BY Dra stars, are an essential class of variable stars that exhibit periodic brightness variations due to the rotation of a star. These variations are thought to be caused by dark spots on their surfaces, similar to sunspots on the Sun (Lanzafame et al., 2018). BY Dra stars are found in various surroundings, including star-forming regions and open clusters. They are thought to be young, rapidly rotating stars with masses similar to the Sun (Radick et al. 1987) & (Scholz and Eislöffel (2007).

Despite their common occurrence, the exact mechanisms behind the formation and evolution of BY Dra variables are still not fully understood (Chahal, 2022). As a result, the monitoring of BY Dra stars is essential in order to gain a better understanding of this class of variable stars. By studying the brightness variations of these stars over time, researchers can learn more about the processes that shape the evolution of young stars and the role of spots in star formation.

BY Dra stars can be single stars or binary systems, of which 70% are binary systems nearby (Schrijver, 2008). BY Dra stars usually comprise a red dwarf and a G- or K-type companion. Binary BY Dra stars are more chromospherically active than single stars. Spectroscopically, BY Dra systems are said to be close in analogy to RS CVn systems

DOI: 10.5817/OEJV2023-0239

(Chahal, 2022). However, they can be distinguished apart by their luminosity flux as they usually have fainter absolute magnitudes than RS CVn binaries (Chahal, 2022).

BY Dra light curves exhibit periods from a fraction of a day to 120 days (Watson, 2006) with brightness variation commonly exhibiting some irregularity between successive periods. Hence, BY Dra systems display quasi-sinusoidal periodicity owing to rotational modulation combined with gradual changes in their average brightness that are caused by changes in the distribution or location of spotted regions on the star's surfaces (Alekseev, 1999). Some of the BY Dra stars that exhibit chromospheric activity, also show flares similar to those observed on UV Ceti stars.

This research is based on the study of a BY Dra star, GSC 05586-00270 discovered by Brincat (2020). The study of a single star out of many others of the same class is essential because unique information may not be readily evident from studying just a population of stars through a holistic process. As every star has its characteristics, research targeting individual stars is important to identify variations within a particular class of stars that can lead to a deeper understanding of the processes these stars undergo throughout their lives.

1.1 GSC 05586-00270

The star GSC 00586-00270 with coordinates RA 14h 55' 50.76" DECL -12° 28' 15.1" belongs to the BY Dra class, and its variability was discovered by Brincat SM in 2020 (VSX, 2020). This star is also known as 2MASS J14555077-1228150, ATO J223.9613-12.4709, NSVS 16159721, and UCAC4 388-064992. Located in the constellation of Libra, GAIA DR3 derived a radius of 2.1 times that of the Sun and its parallax measurement suggests a distance of 374.2453 pc (Rybizki et al., 2020).

Data submitted to AAVSO International Variable Star database (VSX) by the discoverer provides a phased light curve based on the ASAS-SN survey data retrieved and analysed through the Lomb-Scargle algorithm. A prominent period of 9.1012 days with a magnitude range of 12.07 to 12.30 in the V (Johnson) bandpass (epoch: HJD 2455982.9749) was uncovered. The phased plot (fig. 1) and attributes derived from online professional surveys indicate that GSC 05586-00270 belongs to the BY Dra class of variable stars. The AAVSO International Variable Star database (VSX) officially recognised this star as a new variable star and was given the identifier AUID 000-BMH-248.

DOI: 10.5817/OEJV2023-0239

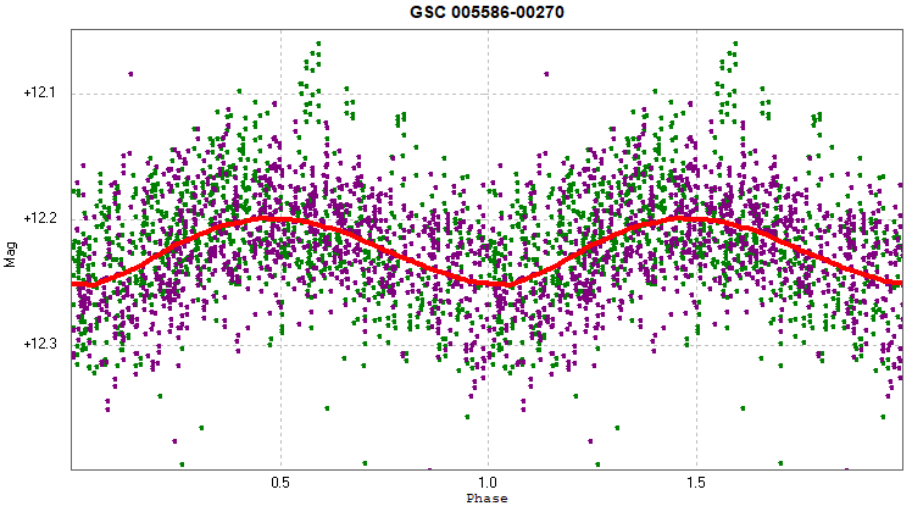

Figure 1: Phased plot with the published period of 9.1012 d based on ASAS-SN survey data. Data points in V are green, while Sloan 'g' data are purple.

Long-term data obtained by the ASAS-SN survey indicated that the star also exhibits long-term variations consistent with the BY Dra class. Other than for the primary period, long-term variations are not often reported in databases. With the knowledge that some of the BY Dra stars also exhibit multiple periods, this study attempts to delve further into the photometric variability of GSC 05586-00270.

2 Observation

The brightness readings of GSC 05586-00270 through different catalogues ranging from the near-infrared to the optical region are shown in Table 1.

Table 1: This is an example of a table. Its caption could be e.g., Summary of observations (or alternatively, Observation log). Columns B,V,R_c,I_c give the number of usable exposures in particular filters.

Catalogue	**Photometric Bands**			**Sources**
GAIA EDR3	G = 11.933234 ± 0.003700	BP = 12.459151± 0.008298	RP = 11.252623 ± 0.007070	Gaia Collaboration. 2020
2MASS	J=10.430 ± 0.024	H = 9.984 ± 0.023	K = 9.836 ± 0.020	Cutri et al. 2003
APASS-DR9	B = 13.176 ± 0.036	V = 12.179 ± 0.043	g = 12.633 ±0.036	Henden et al. 2016

From the data mined from the All-sky Automated Survey for SuperNovae (ASAS-SN) (Kochanek, 2017) and the Zwicky Transient Facility (ZTF) (Bellm, 2014), we have derived

http://oejv.physics.muni.cz
DOI: 10.5817/OEJV2023-0239
ISSN 1801-5964

the light curve shown in Fig. 2. The V and 'g' magnitudes were extracted from the ASAS-SN Survey and 'g' magnitudes from the ZTF (ATLAS) sky survey. An offset has been applied to all of the 'g' data to align with V data obtained from the ASAS-SN survey. In order to display the brightness variations over seasonal (annual observing windows), we have colour-coded the data points to provide an insight into the seasonal photometric variations. The light curve encompasses 3326 data points from JD 2455985.1 to 2459840.5, spanning 3855 days (or 10.55 years). A 5-degree polynomial fit suggests an average GSC 005586-00270 magnitude of 12.175 (V Johnson bandpass). The apparent sinusoidal variation shows a long-term period that is discussed further below.

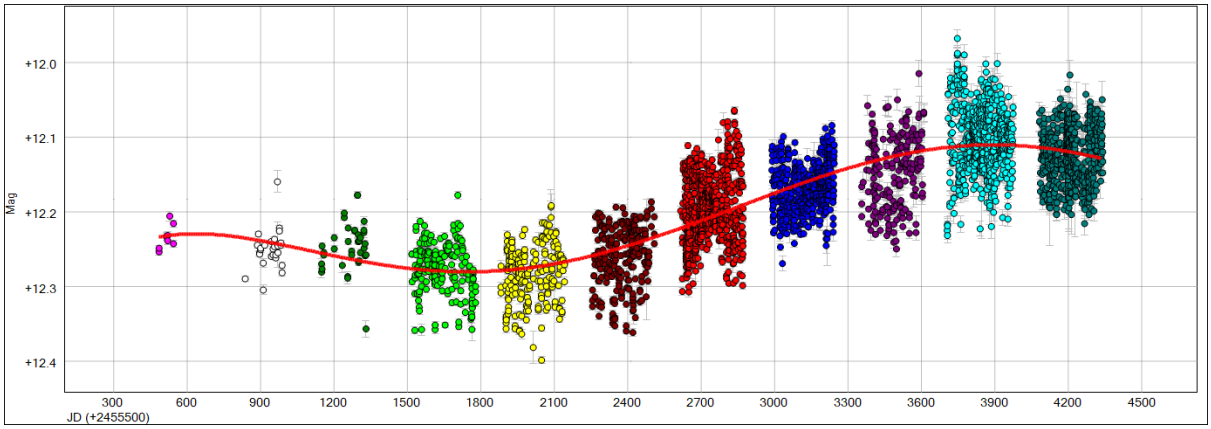

Figure 2: Ten-and-a-half-year light curve, derived from the ASAS-SN and ZTF data showing a long-term sinusoidal variation. Colour coding is attributed to each annual observation window. The red line represents a 5-degree polynomial fit with an average magnitude of 12.175 (V Johnson bandpass).

The light curves panels shown in Fig. 4 show the variation in brightness of GSC 05586-00270 for each observation window from 2015 to 2022. As we had a longer time span of observations than at the time of discovery (fig.1), we investigated whether additional periodicities exist around the rotational period of 9.08 d.

From the data obtained through the ASAS-SN survey, each panel in Fig. 4 displays the photometric variation through the V passband with additional g passband data ("g" filter, based on the Sloan Digital Sky Survey – SDSS, photometric system) that were aligned through an offset to the V standard. The light curves show semi-regular cyclic variability with a varying amplitude that is thought to be due to star spot migration over different latitudes on the star's surface (Hall, 1991).

Through a period search of less than the 120-day maximum rotational period displayed by BY Dra stars (Watson, 2006) using the Generalized Lomb Scargle (GLS), the Phase Dispersion Minimization (PDM), the Fourier (Harris) and the Conditional Entropy (CE) algorithms, we found an additional period of significance with a peak at around 9.5 days. Figure 3 shows the GLS algorithm results that display a prominent secondary peak at the 9.5-day period.

OPEN EUROPEAN JOURNAL ON VARIABLE STARS
http://oejv.physics.muni.cz
DOI: 10.5817/OEJV2023-0239
ISSN 1801-5964

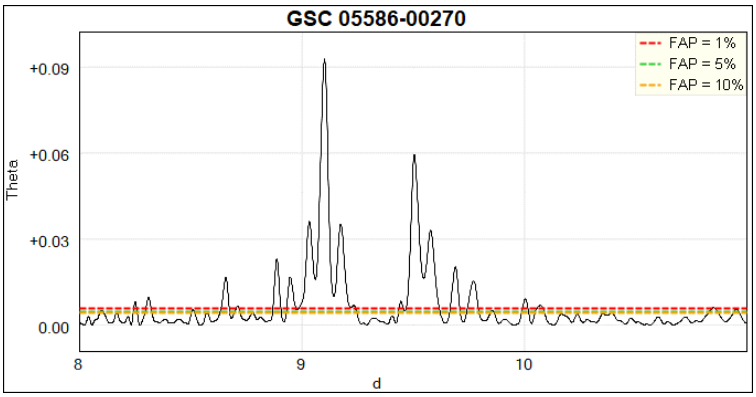

Figure 3: GLS Period search showing the highest peak at 9.1 d and a 9.5 d secondary period.

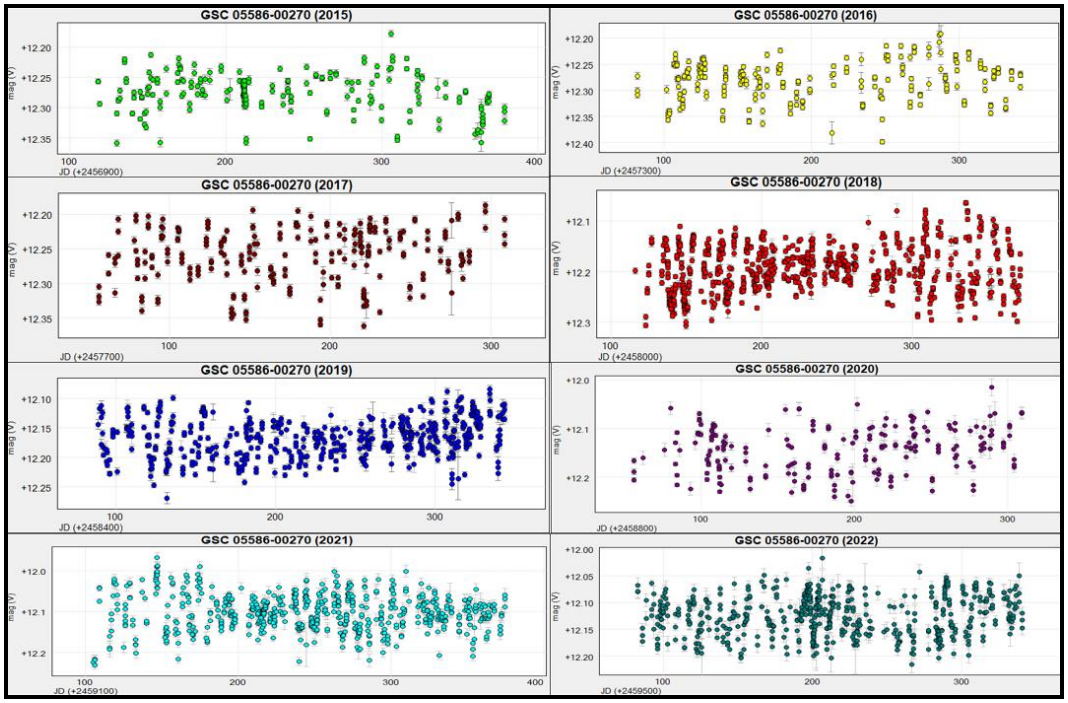

Figure 4: ASAS-SN and ZTF light curves in the V-bandpass showing the variability of GSC 05586-00270 during the annual observation window from 2015 to 2022.

3 Multiple Period Search

The CLEANest algorithm (Foster, 1995) through PERANSO (Paunzen & Vanmunster, 2016) was used to investigate any underlying periodicities in the data further. This algorithm finds periodicities in unequally-spaced data within the power spectrum using the Date Compensated Discrete Fourier Transform (DCDFT).

DOI: 10.5817/OEJV2023-0239

The results obtained using the CLEANest algorithm that displays the details of the primary and secondary periods are shown in Fig. 5 and Table 2. The algorithm detected other lesser periods, but their Theta value was much lower, and subsequently, phased light curves forcing on these periods did not reveal any coherent data.

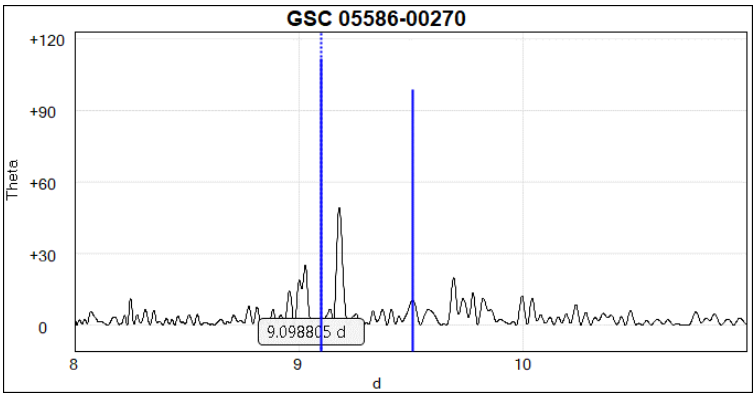

Figure 5: CLEANest spectrum showing a composite graphical representation of two sets of information: (a) the optimal discrete Fourier representation of the data (the so-called discrete spectrum), and (b) the Fourier transform of the residuals (residual spectrum).

Table 2: Multiple Period Search results through the CLEANest algorithm.

Period	**Freq (Hz)**	**Freq Error (Hz)**	**Period (d)**	**Time (error)**	**THETA**
Primary Period	0.10990	0.00002	9.098805	0.001507	111.74
Secondary Period	0.10517	0.00002	9.508168	0.001783	98.67

Figures 6 and 7 are the resultant light curves of the periods in Table 2. Their morphology shows that the phase is coherent and is, therefore real (otherwise, one would see a scattered LC with no distinct cyclic variability.

http://oejv.physics.muni.cz
DOI: 10.5817/OEJV2023-0239

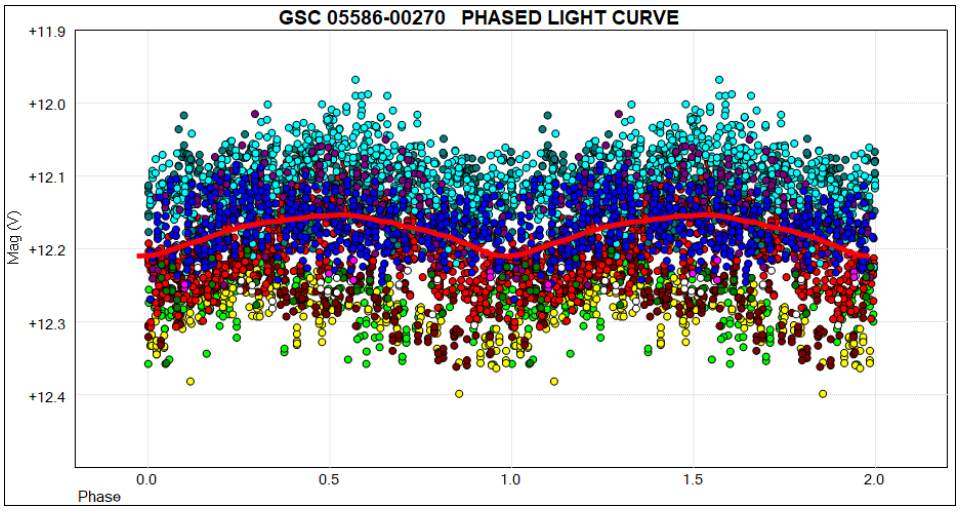

Figure 6: Phased plot of the primary period of 9.098805 d. Epoch = 2455984.22787.

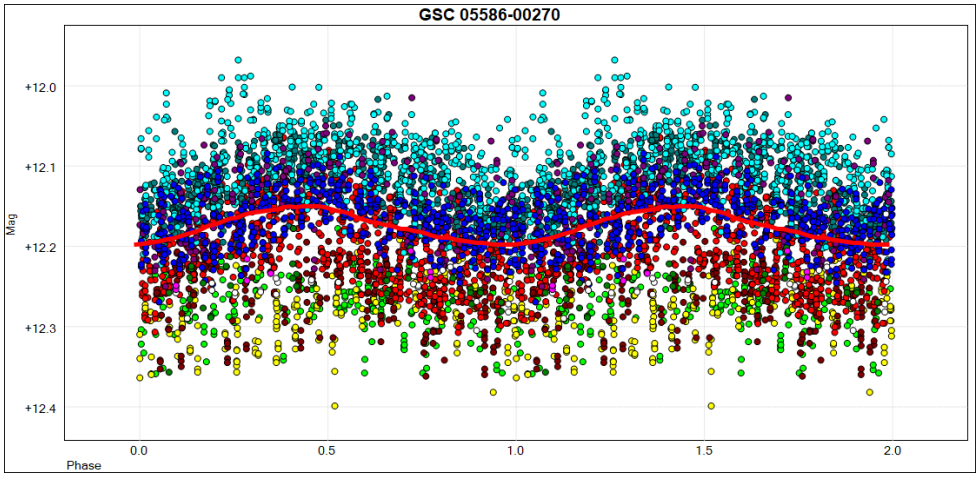

Figure 7: Phased plot of the secondary period of 9.504594 d. Epoch = 2455984.22787.

3.1 Weighted Wavelet Z-Transform Analysis

The Weighted Wavelet Z-Transform (Foster, 1996) method was used to investigate whether the 9.1 d period of GSC 05586-00270 experienced any change in period over time. The WWZ is a time-frequency analysis method that explores both the frequency domain and the time domain by utilising a spectral analysis method to identify periodic signals in data. It is similar to the Lomb-Scargle algorithm but includes a weighting factor that adjusts the importance of different frequencies based on the characteristics of the data (Foster, 1996).

Whereas traditional period analysis methods produce a plot of some response (e.g., power) as a function of either time or frequency, the WWZ method produces output for a range of frequencies and time, resulting in a 3D plot with the X axis representing time, the Y

DOI: 10.5817/OEJV2023-0239

axis representing frequency, and a colour (Z axis) used to plot the WWZ response. This allows for a more comprehensive analysis of the data and the identification of patterns or trends over time and frequency.

The WWZ results shown in Fig. 8 indicate that GSC 05586-0270 9-day period was not evenly dominant throughout 2015-2022. It displays an absence of the prominent period (lesser WWZ value) from JD 2456000 to 2457000. This may be attributed to the limited number of observations during this period. As data by the ASAS-SN and ZTF surveys acquisition improved over time, the algorithm could extract meaningful data that displayed the incidence of the 9 days. The WWZ response in Fig. 8 shows that the 9-day period was most prominent at around JD 2459300. The results also indicate that there were times when the main period diminished its prominence. This may be due to the evolution of starspots, which are known to be dynamic (Chahal, 2022). To this end, even though it has not been so prominent at certain times, the primary period has always reemerged with the same period of around 9.1 days. In conclusion, the WWZ-Transform analysis yielded no evidence of GSC 05586-00270 period change.

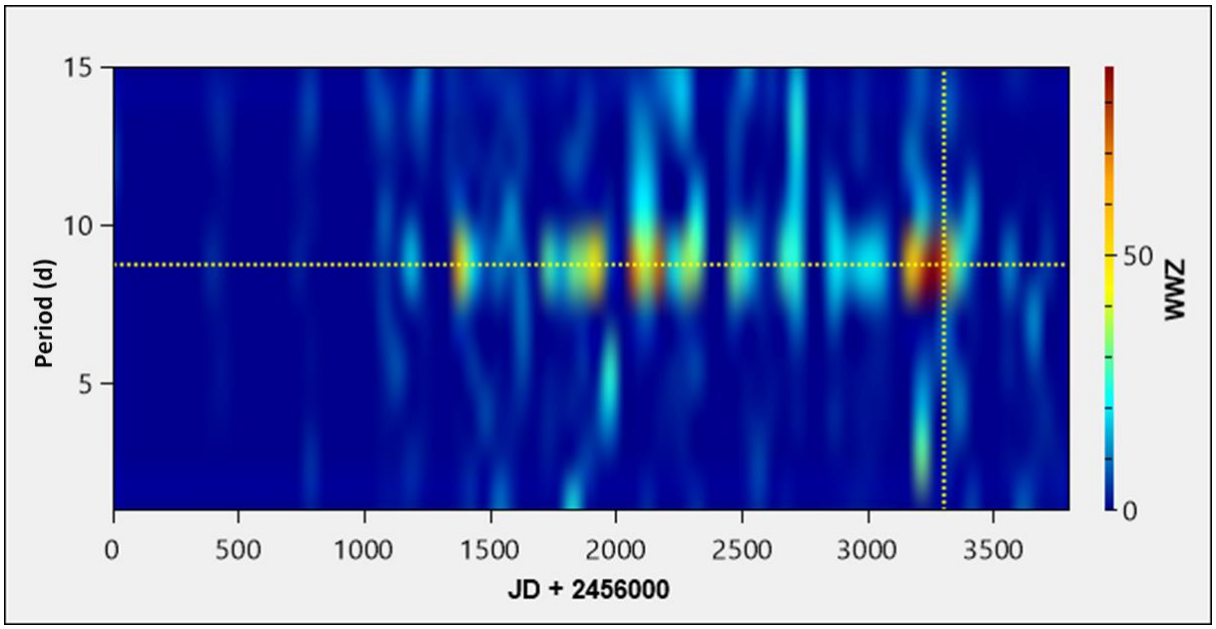

Figure 8: Weighted Wavelet results of GSC 05586-00270 showing a stable 9.1 d period over time.

4 Colour Index

Observations through the V (Johnson) and I (Cousins) bandpass were acquired from Flarestar Observatory through a five-night observation run spread over 13 days. The resultant light

DOI: 10.5817/OEJV2023-0239

curve revealed the typical variability of GSC 05586-00270 through the 9.1 days. The V and I data presented in Table 2 are based on the average of multiple photometric observations per night in each bandpass to improve the accuracy of the readings. These observations enabled us to determine the observed Color Index (CI) of GSC 05586-00270 and different phases.

Table 3: Colour Index derived from V-I data.

JD	Mag (V)	Error	Mag (I)	Error	Color Index
2457893.438	12.28228	0.0277	11.16479	0.0856	1.11749
2457898.398	12.16452	0.0306	11.07395	0.0850	1.09057
2457901.424	12.22535	0.0291	11.11519	0.0861	1.11016
2457903.398	12.28911	0.0278	11.16995	0.0811	1.11916
2457906.342	12.16650	0.0236	11.0835	0.0816	1.08300

Before applying the dereddening coefficients, a color index (V-I) change of GSC 05586-00270 was observed to fluctuate from 1.08300 to 1.11916. These values were based on data acquired over 5 nights, during which several observations acquired each night were averaged to obtain more accurate results. The amount of interstellar extinction through the NASA/IPAC Extragalactic Database - Coordinate Transformation and Galactic Extinction Calculator (NASA/IED, 2015) was then calculated to obtain the dereddened colour index shown in equations I and II.

$$E(B–V) = AB – Av = 0.283 – 0.208 = 0.075 \quad \text{(I)}$$

and

$$E(V–I) = Av– AI = 0.208 – 0.118 = 0.09 \quad \text{(II)}$$

Using the derived (V–I) colour index and assuming an error of 0.02 for Av and Ar (Schlafly and Finkbeiner, 2011), the dereddened colour index for GSC 05586-00270 was determined as follows:

$$(V–I)Min = (V–I) – E(V–I) = (1.119 – 0.090) \pm 0.03 = 1.029 \pm 0.03$$
$$(V–I)Max = (V–I) – E(V–I) = (1.090 – 0.090) \pm 0.03 = 1.000 \pm 0.03$$

According to Mamajek (2019), the average colour index (derived from the average CI at maximum and minimum as 1.014) of our V–Ic values fits with spectral type K3 V that, suggests an effective mean temperature of ~4830 K. GSC 05586-00270 varies through a temperature range of 406 ± 42.2 K. Figure 9 shows that there is a good correlation between the phase of the star and the CI Index.

OPEN EUROPEAN JOURNAL ON VARIABLE STARS
http://oejv.physics.muni.cz
DOI: 10.5817/OEJV2023-0239
ISSN 1801-5964

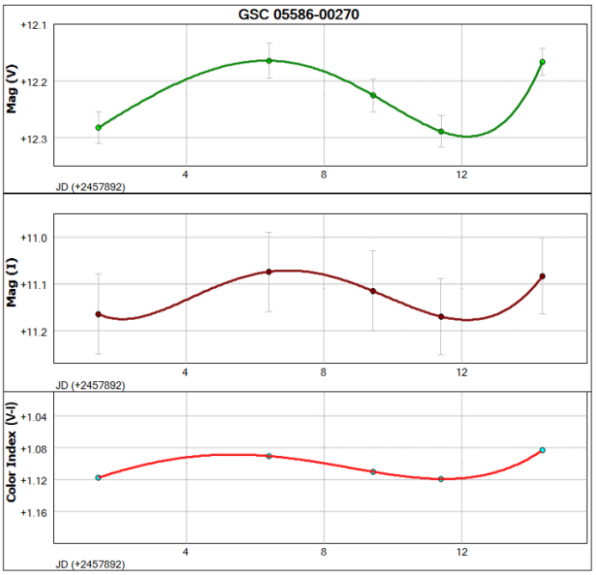

Figure 9: V and I light curves showing the observed Color Index (V-I) of GSC 05886-00270 over five nights. The CI graph displays a correlation to the phase of the star. The suggestive line between data points is a polynomial at the 5th level.

Our results show that the effective mean temperature of GSC 05586-0027 is ~4830 K, which aligns with those derived from the catalogue data shown in Table 4. The temperature results should be taken in the context that a change in IC has been observed, and thus there is a temperature change as the star goes through its phases.

Table 4: Temperature of GSC05586-00270 from Survey data.

Survey	**Star ID**	**Effective Temperature (K)**	**Reference**
The GAIA EDR3 catalogue	6312986026809931520	4500	Gaia Collaboration, (2020)
TESS Input Catalog Ver 8.2	388-064992 (UCAC 4)	4983	Paegert, (2021)
ATLAS all-sky stellar ref. catalog, ATLAS-REFCAT2	6312986026809931520 (Gaia DR2)	4816	Tonry, (2018)

5 Long-Term Variability

The data acquired by the ASAS-SN survey showed a 5th-degree polynomial fit that shows a possible cyclic variation over a time scale of years. The data in Figure 10 was analysed through a Generalised Lomb-Scargle algorithm that shows a period of 4676 days (12.8 years) based on an observations period range of 3607 days (9.87 years). Due to the lack of data

available on longer timescales, this period can only be considered an indicative period, as insufficient information is available to determine the period with certainty. The resultant plot from the 3607-day phased light curve is shown in Figure 12.

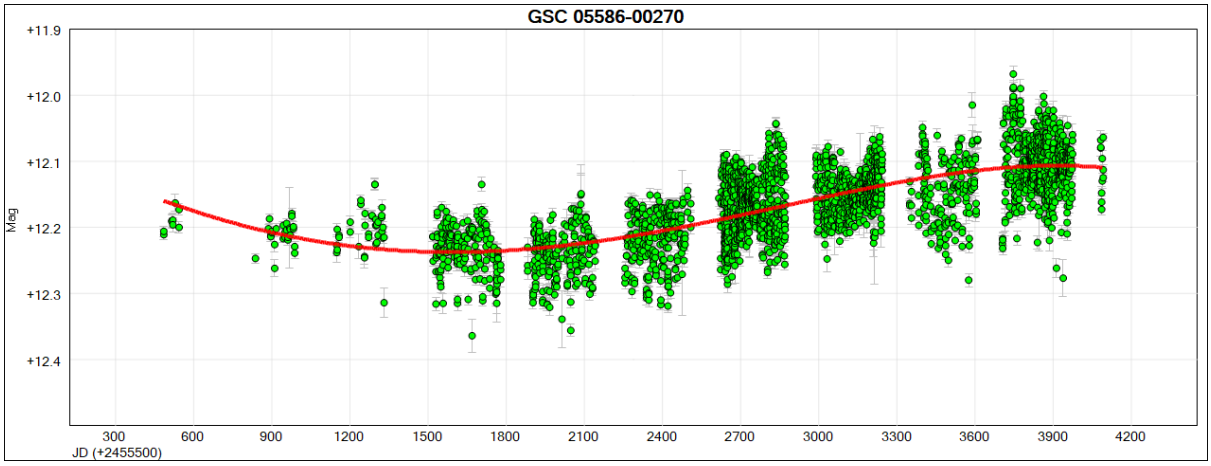

Figure 10: Data obtained by the ASAS-SN survey shows a possible cyclic variation over a time scale of many years.

The ANOVA, PDM, GLS, and FALC (Harris) algorithms were used to search for a long-term period activity cycle in GSC 05586-00270. These algorithms generated different results partly due to the algorithm strength when dealing with gaps in the data. Despite the limited time span of the available data, we have determined a provisional long-term period to be 4442 ± 1048 days based on the calculated mean of the output from these algorithms (Table 5).

Figure 11 shows the Periodogram generated by the Generalized Lomb-Scargle (GLS), as shown in Table 5. GLS results show a peak with a period of 4568 days with an open-ended depiction indicating that the period could be on more extended time frames. This was in line with our expectations as the temporal data range available is somewhat restricted to be less than the derived period.

Table 5: Long-term period activity cycle of GSC 05586-00270.

	Period (d)	**Error (d)**	
ANOVA	4654.470	4654.470	
FALC (Harris)	4530.540	192.942	
GLS	4568.122	4568.122	
PDM	4017.005	2672.311	
Mean	4442.5344	Error standard deviation: 2096.131	Standard error of the mean: 1048.065

OPEN EUROPEAN JOURNAL ON VARIABLE STARS
http://oejv.physics.muni.cz
DOI: 10.5817/OEJV2023-0239
ISSN 1801-5964

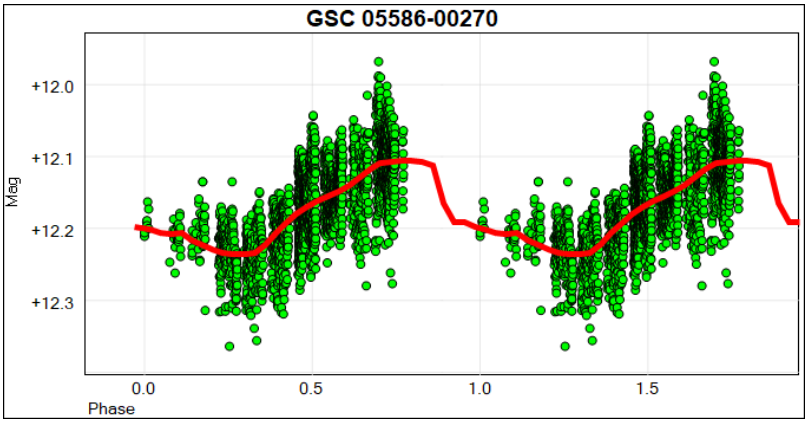

Figure 12: Polynomial fit to the phased plot data based on the 4676-day period.

6 The search for flares over GSC 05586-000270

BY Dra stars are known to be active and prone to display flaring activity (Neff, 1989; Flores Soriano, 2017; Vida, 2009), and this makes them an ideal target for flare studies. Table 6 shows the image dataset taken by the observatories aimed at detecting flares on GSC 05586-000270. They accounted for well over 4900 images taken with less than one minute cadence using a C filter spread over many different nights. Although flares are best visible in the B-bandpass, significant flaring events would still be detectable through C-filtered observations.

Table 6: Image dataset taken by the observatories aimed at detecting flares on GSC 05586-000270 during the period of 2020/2021 using a clear filter.

Observatory/Location	**Telescope Aperture (m)**	**Observation runs**	**Images / Exp^{sec}**	**Effective Monitoring (Hrs.)**
Znith / Malta	0.20	11	668 / 60	11.133
Flarestar / Malta	0.25	16	854 / 60	14.233
Antares / Malta	0.27	17	2233 / 60	37.216
Manikata / Malta	0.20	5	331 / 60	5.516
Tacande / Spain	0.55	10	880 / 40	4.884
Total	--	44	4966	76.97

The processing of clear-filtered throughout the observation period revealed only two low-amplitude flaring events photometry revealed two low-amplitude flaring events recorded on 2020 July 11 (fig. 13) and on August 18 (fig. 14) from Antares and Flarestar Observatories, respectively. Figure 13 shows the event where the star brightness increased

DOI: 10.5817/OEJV2023-0239

from a quiescence level of 12.145 mag to 12.099 mag (or -0.046) in less than one minute. The second flaring event of 2020, August 18 (fig. 14), showed an amplitude of -0.053 mag in less than a minute. Appendices I and II depict the data of these two flaring events.

Flares on BY Dra stars are typically caused by magnetic reconnection events, which release a large amount of energy in the form of light and heat emitted across a wide range of wavelengths, particularly towards the ultraviolet and blue-green regions of the spectrum (Balona, 2020) and (de Grijs, 2021). In this context, the star's measured flux through clear-filtered photometry is lower than those acquired through B-filtered observations. This suggests that the two low-amplitude flares recorded in our images would have had much higher amplitudes if they were recorded through the B-bandpass.

Due to the limitation of only clear-filtered data available on these events, it was not possible to measure the energy emitted by these flares as this required photometric data from other photometric filters. However, this data can be used to determine the flare frequency of GSC 05586-00270 as one event occurring every 38 h of observation.

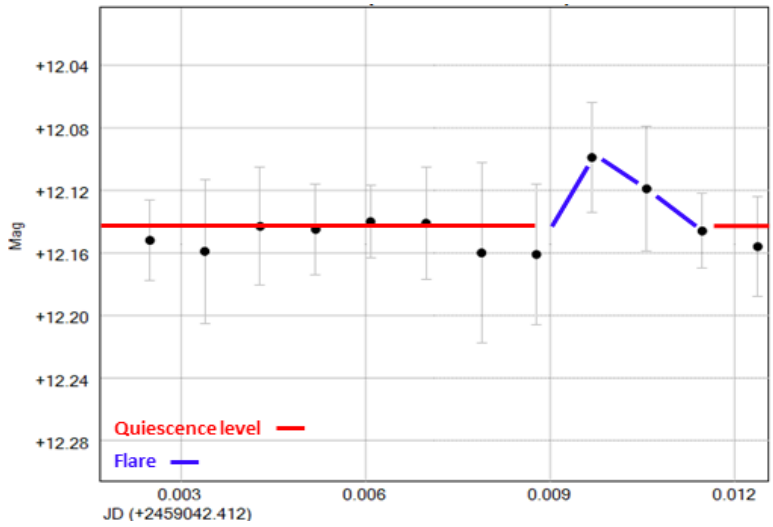

Figure 13: Low-amplitude flare over GSC 05586-00270 recorded on 2020 July 11 using C filter.

DOI: 10.5817/OEJV2023-0239

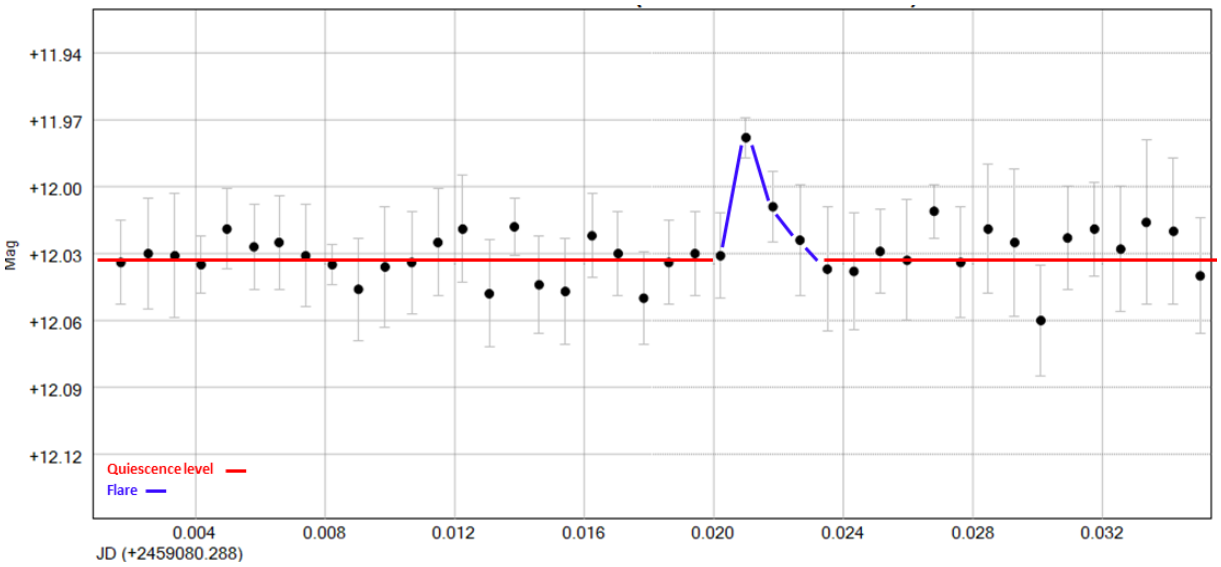

Figure 14: Low-amplitude flare over GSC 05586-00270 recorded on 2020 August 18 using C filter.

7 Is GSC 05586-00270 a single or a binary star?

According to de Grijs and Kamath (2021), approximately 70% of BY Dra class variable stars are close binary systems. With this in mind, we have examined survey data to determine whether GSC 05586-00270 is a binary star system.

Using the stellar parameters from the GAIA DR3 survey data, including the star's apparent magnitude, the absolute magnitude of GSC 05586-00270 was determined to be +4.3. Regarding Chahal (2022; fig. 3), which shows the delineation between single stars and binary ones according to the derived BP-RP and absolute magnitude, we can infer that GSC 05586-00270 belongs to a binary star system. This assumption is supported by the fact that this star exhibits a more complex light curve than a single star.

DOI: 10.5817/OEJV2023-0239

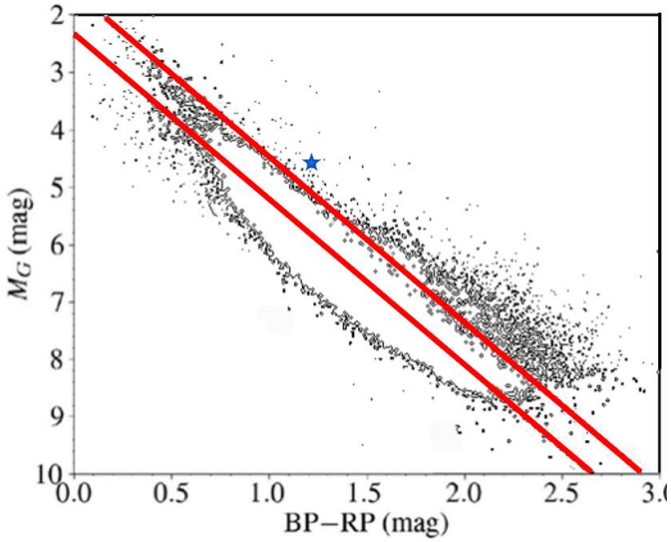

Figure 15: Gaia absolute G-Band against (GBP - GRP) diagram adapted from Chahal (2022). Red line represents equal mass (and luminosity). Binary systems located 0.753 mag above single-star (lower left) isochrone.

Subsequent research has revealed that GSC 05586-00270 has been listed among the stars in the Gaia DR3 Part3—non-single stars catalogue (Gaia Collaboration, 2022). The catalogue data shows that a model was derived for this star that exhibited an SB1 model (single-lined spectroscopic binary star). This entry discloses that the star is a pair of stars orbiting each other, but only one can be detected spectroscopically because the companion star is too faint or possibly has a similar spectrum. The SB1 system has revealed that GSC has an orbital period of 7.545 days.

In retrospect that our data has revealed a rotation period of 9.099 days. These values portray that GSC 05586-00270 has a P*rot*:P*orb* ratio of 5:6. For every five rotations of one star, the system has six orbits. We surmise it is not a tidal-locked situation but close to a spin-orbit resonance. Spin-orbit resonances can occur when there are strong gravitational interactions between the objects in a system, and they can affect the stars' shape, temperature, and magnetic activity (Cherkis & Lyutikov, 2021). Hence, the ratio of 5:6 between Prot and Porbit indicates a specific relationship between the rotational and orbital periods of the stars in the GSC 05586-00270 system.

8 Conclusion

In this study, ASAS-SN and ZTF surveys show that GSC 05586-00270, a BY Dra star, has a period of 9.1001 days. Based on additional observations obtained by a group of observatories, the light curve of GSC 05586-00270 an additional period of 9.508168 days, was derived on the basis of GLS, ANOV, and PDM algorithms. Further refinement using the CLEANest algorithm derived a primary period of 9.098805 days.

DOI: 10.5817/OEJV2023-0239

The WWZ algorithm was used to analyse the temporal stability of this primary period. It was found that the periodicity of GSC 05586-00270 may fade at times but continues to maintain an overall 9.1 day-period. This suggests that the primary period of GSC 05586-00270 is relatively stable.

Based on the colour index of GSC 05586-00270 using the V and IR band passes, correlation analysis between the colour index and different phases of the star indicates that the brightness and colour of GSC 05586-00270 may vary systematically as it rotates and undergoes magnetic activity.

Furthermore, a long-term period of ~ 4442 days was identified that might be related to the migration of starspots and other possible external factors, such as a change in spot configuration (Alekseev, 1999). Using statistical data for BY Dra stars from Chahal (2022), we determined that GSC 05586-00270 is likely a binary star system rather than a single star. This suggests that the complexity of GSC 05586-00270's brightness variations may be partly due to the presence of a companion star, which may thus affect the rotation and magnetic activity of GSC 05586-00270.

Overall, these results provide valuable insights into the characteristics and behaviour of GSC 05586-00270, and suggest that it is a complex, magnetically active star with multiple periods of variability over short and long periods. The presence of multiple periods suggests that GSC 05586-00270 is influenced by various factors, including its rotation and magnetic activity, as well as the presence of a companion star. The correlation between the colour index and different phases of the star indicates that the brightness and colour of GSC 05586-00270 may vary systematically as it rotates and undergoes magnetic activity. Furthermore, this study provides evidence of low-amplitude flares emanating from the star at a rate of 1 event every 38 hours. The attributes above indicate that GSC 05586-00270 is a dynamic, binary star system.

Further research is needed to understand the properties and evolution of GSC 05586-00270, especially in identifying additional factors that may influence its behaviour. BY Dra stars are important because they can be used to study the physical processes within them, such as convection, rotation, and magnetic activity. The results obtained on individual BY Dra stars, such as GSC 05586-00270, are deemed valuable because they can provide insight into the unique characteristics of these particular stars. Further studies on GSC 05586-00270 are strongly encouraged, including spectroscopy, physical characteristics, surface gravity, and chemical composition. Interestingly, such studies can also reveal the presence of other objects in the star's environment, such as exoplanets or debris discs.

Acknowledgements: We would like to express our gratitude to Chahal, D., for permitting us to reproduce Figure 15 from their paper, "Statistics of BY Draconis Chromospheric Variable Stars". The diagram presented in Figure X has been instrumental in illustrating an essential aspect of our research, and we appreciate their generosity in allowing us to utilise it in this work. This research made use of the all-sky automated survey for supernovae (ASAS-SN) light curve server v1. 0 and data retrieved from the Zwicky Transient Facility (ZTF). We express our gratitude for granting free access to their databases. We would also like to acknowledge NASA/IED 2015. The NASA/IPAC Extragalactic Database (NED) is funded by the National Aeronautics and Space Administration and operated by the California Institute of Technology.

DOI: 10.5817/OEJV2023-0239

References

Alekseev, I.Y. 1999, Bull. Crime. Astrophys. Obs. 1999, 95, 69, 1999BCrAO..95...69A
Balona, L. A. 2020, arxiv:2008.06305, 2020arXiv200806305B
Bellm, E. C. 2014, arxiv:1410.8185, arxiv:1410.8185
Brown, A. G. A., et al. 2018, A&A, 616, A1, 2018A&A...616A...1G
Chahal, D., et al. 2022, MNRAS, 514, 4932, 2022MNRAS.514.4932C
Cherkis, S. A., & Lyutikov, M. 2021, ApJ, 923, 13, 2021ApJ...923...13C
Cutri, R. M., et al. 2003, VizieR online data catalog, II-246. 2003yCat.2246....0C
Flores Soriano, M., & Strassmeier, K. G. 2017, A&A, 597, A101, 2017A&A...597A.101F
Foster, G. 1995, AJ, 109, 1889, 1995AJ....109.1889F
Foster, G. 1996, AJ, 112, 1709, 1996AJ....112.1709F
de Grijs, R, & Kamath, D. 2021, Stellar Chromospheric Variability. Universe; 7(11), 440, https://doi.org/10.3390/universe7110440
Gaia Collaboration. 2020, Early Data Release 3, EDR3
Hall, D. S. 1991, Learning about Stellar Dynamos from Long–term Photometry of Starspots. In International Astronomical Union Colloquium (Vol. 130, pp. 353-369). Cambridge University Press, 1991LNP...380..353H
Henden, A. A., et al. 2016, VizieR Online Data Catalog, 2336, 2016yCat.2336....0H
Kochanek, C. S., et al. 2017, PASP, 129, p.104502, 2017PASP..129j4502K
Lanzafame, A. C., et al. 2018, A&A, 616, A16,2018A&A...616A..16L/
Mamajek, E. 2019, "A Modern Mean Dwarf Stellar Color and Effective Temperature Sequence", available from http://www.pas.rochester.edu/~emamajek/EEM_dwarf_UBVIJHK_colors_Teff.txt Accessed Jan 2023.
Neff, J. E., Walter, F. M., Rodono, M., & Linsky, J. L. 1989, A&A, 215, 79, 1989A&A...215...79N
Paegert, M., et al. 2021, VizieR Online Data Catalog, IV-39, 2022yCat.4039....0P
Paunzen, E., & Vanmunster, T. 2016, Astronomische Nachrichten, 337, 239, 2016AN....337..239P
Radick, R. R., et al. 1987, ApJ, 321, 459, 1987ApJ...321..459R
Rybizki, J., et al. 2020, PASP, 132, 074501, 2020PASP..132g4501R
Schlafly, E. F., & Finkbeiner, D. P. 2011, ApJ, 737, 103, 2011ApJ...737..103S
Schrijver, C.J., & Zwaan, C. 2008, Solar and Stellar Magnetic Activity, Cambridge University Press: Cambridge, 2008ssma.book.....S
Scholz, A., & Eislöffel, J. 2007, MNNRAS, 381, 1638, 2007MNRAS.381.1638S
Tonry, J. L., et al. 2018, ApJ, 867, 105, 2018ApJ...867..105T
Vida, K., et al. 2009, A&A, 504, 1021, 2009A&A...504.1021V
VSX, 2020, https://www.aavso.org/vsx/index.php?view=detail.top&oid=1545396
Watson, C. L., Henden, A. A., & Price, A. 2006. Society for Astronomical Sciences Annual Symposium, 25, 47, 2006SASS...25...47W

DOI: 10.5817/OEJV2023-0239

APPENDIX I

Observations of flare observed on 2020 July 11. Magnitude (Mag.) is CV: unfiltered with V zero point.

JD	Mag.	Error	Remarks
2459042.406389	12.139	0.024	Data set quiescence at 12.145 (CV)
2459042.407292	12.165	0.026	
2459042.408194	12.129	0.028	
2459042.409097	12.139	0.022	
2459042.409988	12.154	0.036	
2459042.410903	12.144	0.025	
2459042.411794	12.131	0.021	
2459042.412697	12.143	0.021	
2459042.413588	12.127	0.022	
2459042.414491	12.152	0.026	
2459042.415382	12.159	0.046	
2459042.416285	12.143	0.038	
2459042.417187	12.145	0.029	
2459042.418079	12.14	0.023	
2459042.418981	12.141	0.036	
2459042.419884	12.16	0.058	
2459042.420776	12.161	0.045	
			Flare! Amp. 0.046
2459042.421678	12.099	0.035	Duration: 240 sec.
2459042.422569	12.119	0.04	
2459042.423472	12.146	0.024	
2459042.424375	12.156	0.032	End of observation run

DOI: 10.5817/OEJV2023-0239

APPENDIX II

Observations of flare observed on 2020 August 18. Magnitude (Mag.) is CV: unfiltered V zero point.

JD	Mag.	Error	Remarks
2459080.288	12.038	0.02	Quiescence at 12.031 (CV)
2459080.289	12.044	0.018	
2459080.290	12.034	0.019	
2459080.291	12.03	0.025	
2459080.291	12.031	0.028	
2459080.292	12.035	0.013	
2459080.293	12.019	0.018	
2459080.294	12.027	0.019	
2459080.295	12.025	0.021	
2459080.295	12.031	0.023	
2459080.296	12.035	0.009	
2459080.297	12.046	0.023	
2459080.298	12.036	0.027	
2459080.299	12.034	0.023	
2459080.299	12.025	0.024	
2459080.300	12.019	0.024	
2459080.301	12.048	0.024	
2459080.302	12.018	0.013	
2459080.303	12.044	0.022	
2459080.303	12.047	0.024	
2459080.304	12.022	0.019	
2459080.305	12.03	0.019	
2459080.306	12.05	0.021	
2459080.306609	12.034	0.019	
2459080.307419	12.03	0.019	
			Flare! Amp of Flare 0.053
2459080.308206	12.031	0.019	Duration: 120 sec
2459080.308993	11.978	0.009	
2459080.309826	12.009	0.016	
2459080.310660	12.024	0.025	
2459080.311505	12.037	0.028	
2459080.312326	12.038	0.026	
2459080.313137	12.029	0.019	
2459080.313970	12.033	0.027	
2459080.314803	12.011	0.012	
2459080.315625	12.034	0.025	
2459080.316470	12.019	0.029	
2459080.317292	12.025	0.033	
2459080.318102	12.06	0.025	
2459080.318924	12.023	0.023	
2459080.319757	12.019	0.021	

DOI: 10.5817/OEJV2023-0239

2459080.320567	12.028	0.028
2459080.321354	12.016	0.037
2459080.322199	12.02	0.033
2459080.323021	12.04	0.026